

Network Higher-Order Structure Dismantling

Peng Peng ¹, Tianlong Fan ^{2,*} and Linyuan Lü ^{1,2,*}

¹ Institute of Fundamental and Frontier Studies, University of Electronic Science and Technology of China, Chengdu 611731, China; peng_p@std.uestc.edu.cn

² School of Cyber Science and Technology, University of Science and Technology of China, Hefei 230026, China

* Correspondence: tianlong.fan@ustc.edu.cn (T.F.); linyuan.lv@ustc.edu.cn (L.L.)

Abstract: Diverse higher-order structures, foundational for supporting a network’s “meta-functions”, play a vital role in structure, functionality, and the emergence of complex dynamics. Nevertheless, the problem of dismantling them has been consistently overlooked. In this paper, we introduce the concept of dismantling higher-order structures, with the objective of disrupting not only network connectivity but also eradicating all higher-order structures in each branch, thereby ensuring thorough functional paralysis. Given the diversity and unknown specifics of higher-order structures, identifying and targeting them individually is not practical or even feasible. Fortunately, their close association with k -cores arises from their internal high connectivity. Thus, we transform higher-order structure measurement into measurements on k -cores with corresponding orders. Furthermore, we propose the Belief Propagation-guided Higher-order Dismantling (BPHD) algorithm, minimizing dismantling costs while achieving maximal disruption to connectivity and higher-order structures, ultimately converting the network into a forest. BPHD exhibits the explosive vulnerability of network higher-order structures, counterintuitively showcasing decreasing dismantling costs with increasing structural complexity. Our findings offer a novel approach for dismantling malignant networks, emphasizing the substantial challenges inherent in safeguarding against such malicious attacks.

Keywords: complex networks; higher-order structures; higher-order structure dismantling



Citation: Peng, P.; Fan, T.; Lü, L. Network Higher-Order Structure Dismantling. *Entropy* **2024**, *26*, 248. <https://doi.org/10.3390/e26030248>

Academic Editor: José F. F. Mendes

Received: 19 January 2024

Revised: 5 March 2024

Accepted: 5 March 2024

Published: 11 March 2024



Copyright: © 2024 by the authors. Licensee MDPI, Basel, Switzerland. This article is an open access article distributed under the terms and conditions of the Creative Commons Attribution (CC BY) license (<https://creativecommons.org/licenses/by/4.0/>).

1. Introduction

Given its profound implications in diverse dynamics and optimization problems [1–5], the network dismantling [6,7] persists as a focal point in the realm of network science, commanding substantial scholarly attention. For networks consisting of nodes connected through edges, a prevailing assumption suggests that the structural connectivity of the network stands as a prerequisite for its normal dynamics and functioning [7,8]. As a result, disrupting this connectivity becomes a pivotal pursuit, with the aim of impairing network functionality or destabilizing the intricate dynamics stemming from interconnectivity. In particular, evaluating how network connectivity and functional states respond to network dismantling or attack behaviors can be accomplished by monitoring the condition of the giant connected component (GCC) [8]. Additionally, this monitoring facilitates the assessment of the effectiveness and efficiency of dismantling strategies [9]. Let us refer to this methodology as conventional dismantling.

However, rapidly accumulating research indicates that the paradigm of conventional network dismantling is overly simplified, rendering it inadequate to explain certain common scenarios. For instance, complex functional behaviors can still emerge in many networks with relatively small scales [10,11]. Conversely, even when a large network is dismantled into smaller components, its functionality can still be maintained [12,13]. This is primarily because conventional dismantling often focuses on disrupting the network’s overall connectivity. However, local clusters with high internal connectivity are frequently only mildly affected, especially with certain dismantling methods based on bridge nodes [14], weak nodes [2], and communities [15,16], as well as reinsertion-based

operations [17]. These methods aim to remove these local clusters as a whole to rapidly reduce the size of the GCC, driven by cost considerations. These diverse local clusters often serve as the structural foundation for higher-order interactions, playing a crucial role in supporting local dynamics and the “meta-functions” [18,19]. Even when detached from the GCC, their functionality may still be maintained.

Across the fields of biology [20], neuroscience [21], social systems [22], ecology [23], and engineering [24], higher-order interactions are ubiquitous, referring to interactions involving no fewer than three nodes [25,26]. These interactions cannot be decoupled into a linear combination of pairwise interactions [27–29]. For instance, in brain networks, cliques and cavities formed by brain regions serve as representative structures for local information processing (such as memory and computation) and global information integration, enabling the efficient operation of the brain in a distributed and parallel manner [30]. Clique topologies at the level of neurons also play a crucial role in behaviors such as movement and sleep [31]. In protein–protein interaction networks, collaboration among multiple proteins to fulfill specific functions is prevalent [32,33]. In ecological networks, communities formed by multiple species through predation, dependence, or mutualistic relationships constitute the fundamental building blocks of ecosystems [34,35]. In social systems, whether in social relationships or communication, emergence in the form of modules or communities is common [22,36,37]. In engineering and technological networks, the principle of modular functional organization is widespread, with more complex tasks achieved through their cooperative efforts [24]. These higher-order interactions are often modeled as hypergraphs or simplicial complexes when closure properties are satisfied [19]. Conversely, in networks lacking such higher-order interactions, such as cycle-free networks, complexity emergence is challenging, even with a large scale [38–40].

Therefore, in network dismantling, merely focusing on connectivity is insufficient. It is essential to simultaneously target the disruption of connectivity and the destruction of higher-order structures, prioritizing the dismantling of higher-order structures for a more practical and thorough network dismantling. We refer to this as network higher-order structure dismantling (NHSD). The NHSD represents a more generalized dismantling problem, differing not only from conventional dismantling but also from k -core dismantling [41], which is essentially based on k -core percolation (also known as bootstrap percolation) [42,43]. The differences between NHSD and k -core dismantling primarily lie in their assumptions and dismantling objectives. The assumptions of k -core dismantling stem from percolation theory, assuming that a macroscopic feature of the system is primarily determined by the giant component, and components disconnected from the giant component are considered automatically deactivated. Therefore, the objective of k -core dismantling is to dismantle higher-order k -cores within the giant component. However, in the context of complex networks, given that networks often exhibit significant community characteristics, their functionalities are distributed, and their design principles aim for modular functional components. Even if some components detach from the giant component, they can still function normally. NHSD addresses this complicated situation, aiming not only to disrupt the connectivity of the giant component and the higher-order structures within it, but also to eradicate higher-order structures in all other components.

In addition to thoroughly paralyzing the structure and functionality of networks, the NHSD is closely linked to several studies, including blocking higher-order random walks [44], disrupting higher-order synchronization [45], hindering higher-order spreading [46], and obstructing k -core percolation or k -clique percolation [47], among others.

To address the challenge of higher-order structure dismantling, this paper formalizes this problem and introduces a methodology to address it. We discuss the mathematical relationship between various higher-order structures and k -cores, proposing to utilize the proportion of nodes in different k -cores as an indicator for the extent of disruption in corresponding higher-order structures in the dismantling process. Subsequently, taking the scenario of edge dismantling as an example, we present the Belief Propagation-guided Higher-order Dismantling (BPHD) algorithm, grounded in the belief propagation

ration for the BPHD algorithm comes from the BPD algorithm [49]. In scenarios involving node attacks on the GCC of the network, BPD has demonstrated the capability to induce a catastrophic collapse of the GCC in the late stages of the attack. This can be attributed to the intrinsic nature of BPD as an algorithm for constructing a minimum feedback vertex set, which aims to find the smallest set of nodes that includes at least one node from each cycle in the network [48]. Consequently, when nodes selected by BPD are removed from the network, the network transforms into a forest, leading to an explosively disruptive impact on its scale. Here, “forest” refers to a network consisting solely of disconnected tree-like components. This aligns precisely with the objectives of higher-order dismantling. On the other hand, the outstanding performance of BPD has also been demonstrated through the replica-symmetric mean field theory of the spin-glass model [48].

We generalize the BPD algorithm to the edge dismantling scenario, resulting in the BPHD algorithm. In contrast to node dismantling, where each iteration involves removing all edges adjacent to the target node, edge dismantling, by independently removing one edge at a time, demonstrates greater generality, lower cost, feasibility, and broader applicability. Let the marginal probability p_i^0 , similar to the case of nodes [49], denote the probability that edge i should be prioritized for removal in each iteration. It is determined by the following expression:

$$p_i^0 = \frac{1}{1 + e^x \left[1 + \sum_{k \in \partial i} \frac{(1 - p_{k \rightarrow i}^0)}{p_{k \rightarrow i}^0 + p_{k \rightarrow i}^k} \right] \prod_{j \in \partial i} [p_{j \rightarrow i}^0 + p_{j \rightarrow i}^j]}}, \tag{4}$$

where x is an adjustable reweighting parameter and ∂i is the set of neighboring edges of edge i ; i.e., those edges sharing a node with i . $p_{j \rightarrow i}^0$ and $p_{j \rightarrow i}^j$ represent the probability that edge j is suitable for removal after the removal of edge i and the probability that edge j is suitable to be the root edge of a tree component in the absence of edge i , respectively. Assuming edge i is removed, the two conditional probabilities are determined self-consistently through the following two belief propagation (BP) equations:

$$p_{i \rightarrow j}^0 = \frac{1}{z_{i \rightarrow j}}, \tag{5}$$

$$p_{i \rightarrow j}^i = \frac{e^x \prod_{k \in \partial i \setminus j} [p_{k \rightarrow i}^0 + p_{k \rightarrow i}^k]}{z_{i \rightarrow j}}, \tag{6}$$

where $\partial i \setminus j$ is the edge subset obtained by removing edge j from set ∂i and $z_{i \rightarrow j}$ is a normalization constant determined by

$$z_{i \rightarrow j} = 1 + e^x \prod_{k \in \partial i \setminus j} [p_{k \rightarrow i}^0 + p_{k \rightarrow i}^k] \times \left[1 + \sum_{l \in \partial i \setminus j} \frac{(1 - p_{l \rightarrow i}^0)}{p_{l \rightarrow i}^0 + p_{l \rightarrow i}^l} \right]. \tag{7}$$

Under the Bethe–Peierls approximation, we directly apply the BP equations to edges through an edge-to-node mapping, which is directly reflected in the expressions of marginal probability p_i^0 and the BP equations. In the original node dismantling scenario [49], nodes involved in the most cycles were prioritized for removal, whereas, after the edge-to-node mapping, edges involved in the most cycles are identified and prioritized for removal. On the other hand, structures of higher order entail more nested cycle structures, thereby being preferentially targeted for removal by the BPHD algorithm.

In each iteration, BPHD removes the edge with the highest marginal probability p_i^0 in the current network. We employ the BPHD iteratively to remove edges until reaching the connectivity dismantling target $S_{GCC} \leq C$. At this point, we assess whether the objective of higher-order dismantling has also been met. If so, the dismantling process concludes; otherwise, it continues until Equation (3) is satisfied. It is worth noting an exceptional scenario where BPHD, despite iteratively disrupting all cycles in the network, fails to satisfy

$S_{GCC} \leq C$. In this case, the network transforms into a forest, and our dismantling problem degrades into the conventional dismantling. Here, the strategy involves selecting edges that most rapidly reduce the size of the forest until $S_{GCC} \leq C$ is achieved. The process of dismantling higher-order structures with varying orders by BPHD in an illustrative network is depicted in Figure 2. In terms of time complexity, owing to the efficiency of the Belief Propagation model, the BPHD algorithm is $O(M \ln M)$, with M being the number of edges in the network.

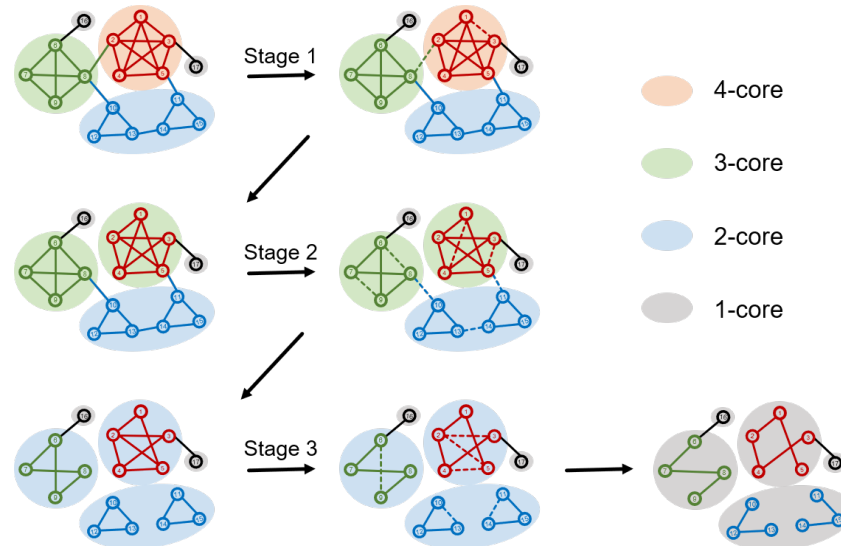


Figure 2. Schematic representation of the BPHD algorithm in the process of dismantling higher-order structures. Here, cliques with varying orders are used to represent different higher-order structures. Nodes of different colors indicate their membership in cliques of different orders in the original network, and shadows of different colors represent the current k -cores with various orders. Dashed edges depict the edges removed by BPHD in the current stage. In Stage 1, a 4-clique is dismantled into a 3-clique, resulting in the disappearance of a 4-core. In Stage 2, two 3-cliques are dismantled, leading to the loss of two 3-cores. In Stage 3, all 2-cliques and cycles are dismantled, ultimately yielding a forest.

4. Results

To evaluate the performance of BPHD, we conducted experiments on six networks, encompassing two classic model networks, Erdős–Rényi (ER) networks [59] and Barabási–Albert (BA) networks [60]. In a BA network with a given number of nodes N and model parameter m , this indicates that each new node connected to m existing nodes and all nodes in the network belong to the m -core. Furthermore, the presence of hub nodes facilitates the straightforward construction of higher-order structures. Additionally, four diverse empirical networks were considered: the protein–protein interaction network of yeast (Yeast) [61], the scientific collaboration network (Collaboration) [62], the email network (Email) [62], and the online social network (Social) [9]. The basic properties of these six networks are outlined in the first three columns of Table 1.

Table 1. The basic attributes of the six networks and the optimal and suboptimal dismantling costs in connectivity dismantling. The first five columns provide the basic attributes about the networks, including the network name, number of nodes (N), number of edges (M), average degree ($\langle k \rangle$), and the maximum order k_{max} of the k -core in the network. The last two columns list the optimal and suboptimal dismantling costs in connectivity dismantling to achieve the dismantling target $C = 0.01N$. The optimal results are indicated in bold.

Network	N	M	$\langle k \rangle$	k_{max}	Dismantling Cost	
					BPHD	Suboptimal
ER	10,000	35,000	7.00	5	0.74	0.84
BA	10,000	49,985	10.00	5	0.82	0.88
Yeast	2375	11,693	9.85	40	0.79	0.84
Collaboration	5094	7515	2.95	7	0.51	0.75
Email	1134	5451	9.61	11	0.80	0.93
Social	2000	16,098	16.10	24	0.85	0.88

Although the NHSD problem is a novel problem, certain existing dismantling algorithms can still serve as valuable benchmarks. Specifically, the connectivity dismantling target $S_{GCC} \leq C$ in Equation (3) aligns completely with the original objectives of Bridgeness (BG) [63] and Edge Betweenness (EB) [64]. Furthermore, three node dismantling strategies renowned for their outstanding performance, namely Collective Influence (CI) [2], Explosive Immunization (EI) [4], and Generalized Network Dismantling (GND) [9], should also be taken into consideration. These three algorithms, as opposed to computing scores for each edge and removing one at a time, individually calculate scores for nodes and remove all adjacent edges of the selected node each time. On the other hand, for the higher-order dismantling target in Equation (3), we still consider BG and EB, as the removal of critical edges identified by them can inflict severe damage on higher-order structures. Additionally, we include a strategy with state-of-the-art performance in k -core dismantling through node removal, Cycle-Tree-Guided-Attack (CTGA) [65]. The detailed definitions of these baseline methods can be found in Section 6.

4.1. Connectivity Dismantling

To facilitate clearer visualization and discussion, we analyze the performance of BPHD separately in connectivity dismantling and higher-order dismantling. Figure 3 demonstrates that the proposed BPHD strategy outperforms baseline algorithms in conventional dismantling, achieving the lowest-cost dismantling. The specific dismantling costs of BPHD and suboptimal methods when reaching the dismantling goal defined in Equation (3) are presented in the last two columns of Table 1. For an ER network with an average degree of seven, BPHD only needs to remove a fraction of 0.74 of the edges, whereas the lowest-cost algorithm among the baselines, the EI algorithm, requires the removal of 0.84. In the case of a BA network with an average degree of 10, indicating higher density, BPHD requires the removal of 0.82, while the suboptimal algorithm necessitates 0.88. Similarly, for the four empirical networks, BPHD performs optimally in all cases. The most significant performance improvement is observed in the Collaboration network, saving 32% of the removal cost compared to the suboptimal algorithm. Additional results for C values of $0.03N$ and $0.06N$ can be found in Figures S1 and S2 in the Supplementary Materials, with consistent conclusions. The results indicate that for various dismantling targets C , the BPHD algorithm can also achieve a conventional dismantling task with lower costs compared to other benchmarks in most cases; only in few cases is the dismantling cost of BPHD higher than benchmarks. In general, the higher the network density, the higher the cost.

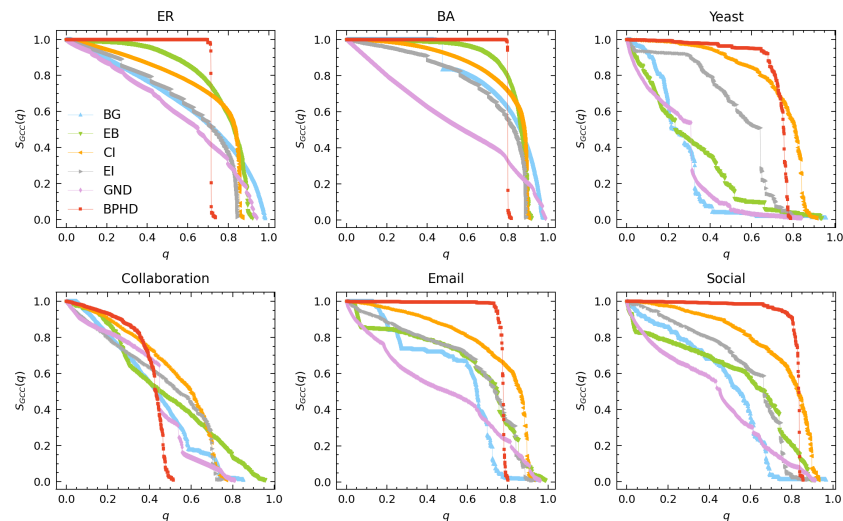


Figure 3. Performance of BPHD in connectivity dismantling. Here, q and $S_{GCC}(q)$ represent the edge removal proportion and the corresponding relative size of GCC in the network, respectively. The dismantling objectives are set as $C = 0.01N$.

Additionally, the dismantling process of BPHD exhibits a distinctive explosive vulnerability pattern [17], where the early-stage GCC's size remains nearly unchanged until reaching a certain threshold, after which it rapidly decreases. This pattern is evident across all networks except for the Collaboration network, contrasting with the continuous decline observed in benchmark algorithms. The BPHD dismantling process demonstrates a pronounced stealthiness, as the removal of crucial edges in the early stages does not significantly disrupt connectivity but focuses more on dismantling higher-order structures, as illustrated in Figure 2. As the network is dismantled into a tree-like structure in the later stages, the GCC undergoes an irreversible collapse suddenly. This combination of early-stage stealthiness and late-stage abruptness poses formidable challenges to network security and robustness.

4.2. Higher-Order Structure Dismantling

Figures 4 and 5 showcase the results of higher-order dismantling achieved by BPHD, where we exemplify the cases of 5-core, 4-core, 3-core, and 2-core. Consistent with Equation (3), we utilized the relative size of k -cores at each order in all branches as a signal for the variation in higher-order structures of corresponding order in dismantling. Figure 4 compares BPHD with two distinguished edge dismantling strategies, BG and EB. Specifically, colors ranging from dark to light correspond to orders from high to low, and all higher-order structures are sequentially eradicated by BPHD, perfectly aligning with the higher-order dismantling objective in Equation (3), in both synthetic and empirical networks. In contrast, EB and BG do not exhibit such efficiency, as various higher-order structures persist in the final stages of dismantling, indicating their inefficacy in higher-order dismantling, especially in empirical networks. Moreover, for each order of higher-order structure dismantling, BPHD incurs the lowest dismantling cost and demonstrates a more pronounced advantage over baseline methods in empirical networks. Additional results for other higher-order dismantling objectives can be found in Figures S3 to S6 in the Supplementary Materials. Overall, even when facing different higher-order dismantling objectives, BPHD can dismantle higher-order structures in the network faster than EB and BG in most cases, only inferior to the baseline algorithms in a small number of cases. Finally, we observe that empirical networks often require the removal of a higher proportion of edges, with the costs for extinguishing higher-order structures at different orders being closer and the discontinuity in size reduction being weaker in the later stages, indicating the stronger robustness of empirical networks compared to synthetic networks. This implies

that there might be robust mechanisms at play in empirical networks that are yet unknown to us.

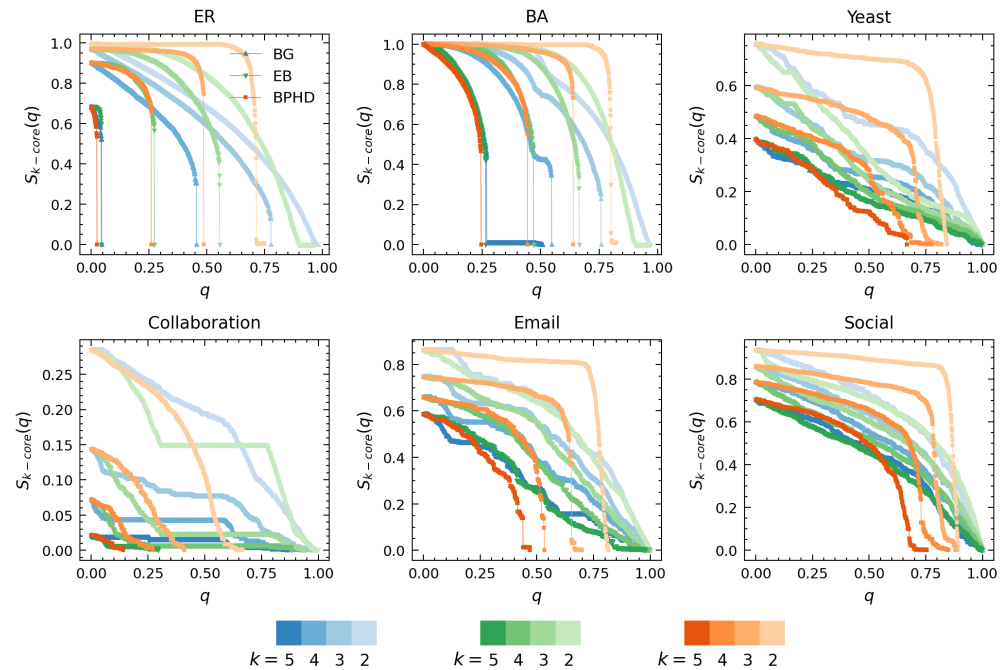


Figure 4. Performance comparison of BPHD with two classical algorithms in higher-order structure dismantling. Here, q and $S_{k-core}(q)$ denote the edge removal proportion and the corresponding proportion of nodes with $k-core$ value equal to k in all branches, respectively. Each color corresponds to a specific algorithm, with shades from dark to light indicating the dismantling results for different orders k . The dismantling objectives are set as $C = 0.01N$ and $H = 0$.

Figure 5 illustrates the performance comparison between BPHD and CTGA. Both BPHD and CTGA are based on the belief propagation model. However, the CTGA algorithm requires setting a specific parameter K for specific-order K -core attack tasks to achieve its optimal attack cost, whereas BPHD is parameter-free. Therefore, the k -core dismantling results of CTGA for orders $k = 5, 4, 3$, and 2 in Figure 5 correspond to the cases where K is set to $5, 4, 3$, and 2 , respectively. In all instances, the BPHD algorithm achieves its optimal attacks against various orders of higher-order structures with a single execution, a remarkable advantage compared to the CTGA algorithm. The detailed dismantling costs for BPHD and CTGA across different orders of k -core are presented in Table 2.

We observe that BPHD outperforms CTGA in the dismantling of k -cores at various orders, demonstrating lower dismantling costs, except for the Yeast and Collaboration networks. This implies that the edges identified by the NPHD algorithm are genuinely important, contributing to the integrity of higher-order structures at various orders. Moreover, in terms of dismantling patterns, BPHD exhibits a more pronounced explosive vulnerability, especially at lower orders. Some of the differences between BPHD and CTGA can be attributed to CTGA’s focus on node dismantling, removing all adjacent edges of the target node in each iteration. However, comparing CTGA with the results of BG and EB in Figure 5, CTGA’s advantages in higher-order dismantling are evident.

In contrast to conventional dismantling (such as BG and EB), higher-order structures become the most vulnerable in higher-order dismantling patterns, requiring the least removal to be effectively dismantled. This is unlike benchmark algorithms where higher-order structures persist until the later stages of dismantling, as evidenced in the empirical networks in Figure 4. The observed higher-order vulnerability and the covert nature of BPHD’s dismantling strategy underscore the need for increased attention to the robustness of higher-order structures within a system. Additional results for other higher-order dismantling objectives can be found in Figures S7–S10 in the Supplementary

Materials. For different dismantling objectives with respect to different orders, BPHD completes higher-order dismantling tasks with lower costs in most cases compared to CTGA. Furthermore, Figure S11 in the Supplementary Materials illustrates two types of dismantling results on a synthetic network with significant community features, where it can be observed that the performance of BPHD remains competitive. For the connectivity dismantling, it can be observed that BPHD does not exhibit superiority, as conventional dismantling algorithms are tailored for such community structures, effectively considering community characteristics and selectively removing inter-community edges. Conversely, for the higher-order dismantling, BPHD demonstrates significant advantages over BG and EB, comparable to the performance of CTGA.

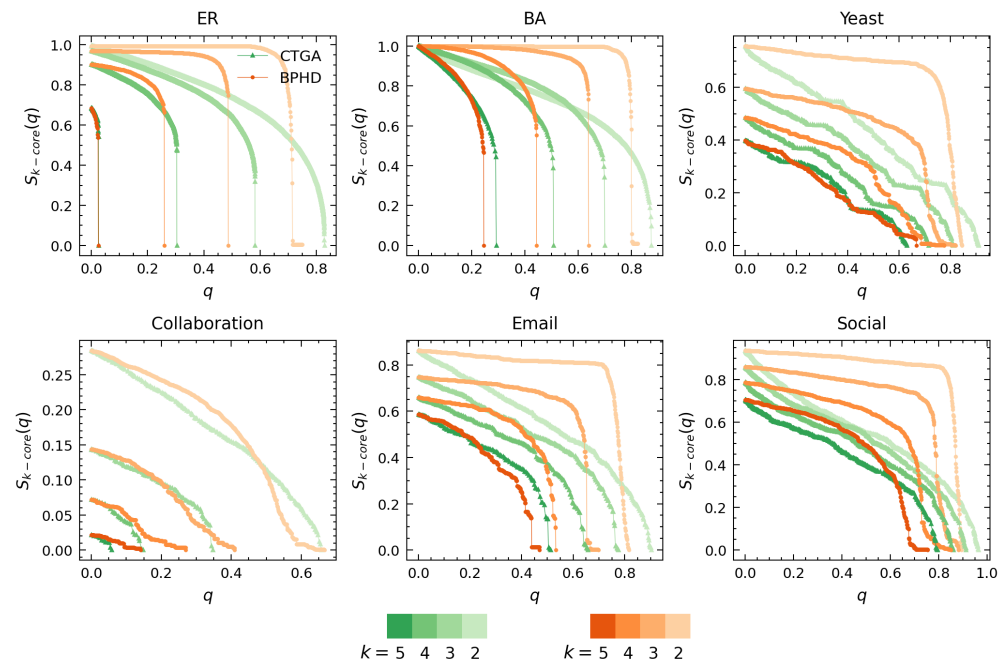


Figure 5. Performance comparison of BPHD with the CTGA algorithm in higher-order structure dismantling. Here, q and $S_{k-core}(q)$ denote the edge removal proportion and the corresponding proportion of nodes with $k-core$ value equal to k in all branches, respectively. Each color corresponds to a specific algorithm, with shades from dark to light indicating the dismantling results for different orders k . The dismantling objectives are set as $C = 0.01N$ and $H = 0$.

Table 2. The dismantling costs of BPHD and CTGA for higher-order structure dismantling at different orders. Specifically, each fraction represents the proportion of edges that need to be removed in the corresponding k -core dismantling to achieve the dismantling targets $C = 0.01N$ and $H = 0$. The optimal results in each column are indicated in bold.

Network	Dismantling Cost							
	2-Core		3-Core		4-Core		5-Core	
	BPHD	CTGA	BPHD	CTGA	BPHD	CTGA	BPHD	CTGA
ER	0.75	0.83	0.49	0.58	0.26	0.30	0.02	0.03
BA	0.82	0.76	0.64	0.70	0.44	0.51	0.25	0.29
Yeast	0.84	0.91	0.82	0.81	0.77	0.71	0.67	0.63
Collaboration	0.78	0.66	0.39	0.35	0.25	0.15	0.13	0.06
Email	0.82	0.90	0.70	0.78	0.53	0.66	0.47	0.51
Social	0.89	0.96	0.88	0.91	0.85	0.86	0.75	0.80

5. Conclusions and Discussion

The higher-order structures within networks play a crucial role in maintaining network architecture, functionality, and giving rise to diverse complex dynamics, garnering

attention across various domains. However, their vulnerability and dismantling problems, closely tied to the former, have not received sufficient consideration. In this paper, we introduce the network higher-order structure dismantling problem, building upon connectivity dismantling and specific k -core dismantling, and underscore the importance of completely disrupting all higher-order structures within all branches of a network. Given the diversity and, in many cases, the unknown specifics of higher-order structures, monitoring the response of each individual structure to dismantling algorithms is often inefficient and, in some instances, unfeasible. Fortunately, the strong internal connectivity of most higher-order structures establishes a close association with the corresponding k -cores. We demonstrate this tight relationship, thereby simplifying the problem of evaluating the efficiency of higher-order dismantling algorithms by monitoring the changes in the k -core values of all nodes. Consequently, we devise a universal framework for higher-order structure dismantling.

Furthermore, we propose an efficient algorithm for higher-order structure dismantling, BPHD, based on belief propagation. Compared to baseline methods, BPHD achieves minimal edge removal cost, maximizing connectivity dismantling and ensuring the complete eradication of all higher-order structures of order two and above. It ultimately transforms the network into a forest, eliminating the possibility of sustaining any complex dynamics or functionality.

BPHD exposes an extraordinary fragility of the network core in higher-order structure attacks. It achieves highly efficient dismantling of the highest-order structures with minimal cost, and, remarkably, higher-order structures collapse earlier as their order increases. Additionally, both diverse higher-order structures and connectivity can be explosively dismantled, manifesting as an early-stage, imperceptible process, followed by a rapid and irrecoverable collapse in the later stages. This suggests that both the core and periphery of the network exhibit explosive vulnerability, posing significant challenges for network maintenance and defense against malicious attacks.

Theoretical and practical implications of the network higher-order structure dismantling problem are vast, and this will be the focal point of our future endeavors. This approach finds applications in modeling and phase transitions in higher-order percolation [66], interrupting disease propagation on simplicial complex networks [46], minimizing costs in viral marketing, communication disruption in drone swarms [67], as well as the thorough dismantling of criminal networks and terrorist organizations [68].

6. Methods

Bridgeness (BG): Bridgeness [63] is a local index used to measure the significance of an edge in maintaining the global connectivity of a network. For edge $e(u, v)$, its ability to connect the large clusters in the network is defined as

$$B_{e(u,v)} = \frac{\sqrt{S_u S_v}}{S_{e(u,v)}}, \quad (8)$$

where S_u , S_v and $S_{e(u,v)}$ are the sizes of the largest clusters containing node u , node v , and edge $e(u, v)$, respectively.

Edge Betweenness (EB): Edge Betweenness [64] is a centrality measure used to identify the edges that are most important for maintaining the global connectivity of a network. According to the idea that the more shortest paths between pairs of nodes pass through an edge $e(u, v)$, the more important the edge $e(u, v)$ is, the centrality of edge $e(u, v)$ is defined as

$$EB(u, v) = \sum_{s \neq t \in V} \frac{\delta_{st}(u, v)}{\delta_{st}}, \quad (9)$$

where δ_{st} is the number of all shortest paths between node s and node t , and $\delta_{st}(u, v)$ is the number of all shortest paths between node s and node t that pass through edge $e(u, v)$. A larger EB score means greater importance of the edge.

Collective Influence (CI): The CI algorithm [2] identifies the smallest set of influencers by solving the node-based optimal percolation problem. Given the parameter ℓ , the value of $CI_\ell(u)$ of node u in the network is defined as follows:

$$CI_\ell(u) = (k_u - 1) \sum_{v \in \partial\text{Ball}(u, \ell)} (k_v - 1), \tag{10}$$

where k_u is the degree of node u and $\partial\text{Ball}(u, \ell)$ denotes the set of nodes in the network whose shortest path length to u is ℓ . Here, we set ℓ to be 3.

Explosive Immunization (EI): The EI algorithm [4] is a method used to interrupt the spread of infection in a network. It combines the explosive percolation (EP) paradigm with the idea of maintaining a fragmented distribution of clusters. This algorithm heuristically utilizes two node scores, $\sigma_u^{(1)}$ and $\sigma_u^{(2)}$, to estimate a node’s ability to interrupt infection propagation at two phases, which are defined as follows:

$$\sigma_u^{(1)} = k_u^{(\text{eff})} + \sum_{\mathcal{C} \subset \mathcal{N}_u} (\sqrt{|\mathcal{C}|} - 1). \tag{11}$$

The first term $k_u^{(\text{eff})}$ is the effective degree of node u , which is determined self-consistently from the original degree k_u :

$$k_u^{(\text{eff})} = k_u - L_u - M_u \left(\left\{ k_v^{(\text{eff})} \right\} \right), \tag{12}$$

where L_u and M_u are the number of leaf and hub nodes in the vicinity of u , respectively. During the iteration, nodes with effective degree $k_v^{(\text{eff})} \geq K$ are regarded as hub nodes for a suitably chosen constant K . Here, we set K to be 6. The second term is determined by the size $|\mathcal{C}|$ of cluster \mathcal{C} in the set \mathcal{N}_u of all clusters linked to u .

As the percolation process proceeds, some harmful nodes identified by $\sigma_u^{(1)}$ become harmless. To distinguish the influence of nodes more accurately, the EI algorithm uses $\sigma_u^{(2)}$ to evaluate the influence of nodes in Phase 2.

$$\sigma_u^{(2)} = \begin{cases} \infty & \text{if } \mathcal{G}(q) \not\subset \mathcal{N}_u, \\ |\mathcal{N}_u| & \text{else, if } \arg \min_u |\mathcal{N}_u| \text{ is unique,} \\ |\mathcal{N}_u| + \epsilon |\mathcal{C}_2| & \text{else.} \end{cases} \tag{13}$$

Here, $\mathcal{G}(q)$ is the largest cluster as qN nodes are removed, $|\mathcal{N}_u|$ is the number of clusters in the neighborhood of u , \mathcal{C}_2 is the second-largest cluster in \mathcal{N}_u , and ϵ is a small positive number (its value is not important provided $\epsilon \ll \frac{1}{N}$). See the original article [4] for more details about the EI algorithm.

Generalized Network Dismantling (GND): The GND algorithm [9] is a method designed to fragment the network into subcritical network components with a minimal removal cost. It is based on the spectral properties of the node-weighted Laplacian operator L_w , and thereby transforms the generalized network dismantling problem into an integer programming problem as shown below.

$$\min_{x = \{x_1, x_2, \dots, x_n\}} \frac{1}{4} x^\top L_w x, \tag{14}$$

subject to

$$\begin{aligned} \mathbf{1}^\top x &= 0, \\ x_i &\in \{+1, -1\}, i \in \{1, 2, \dots, n\}. \end{aligned} \tag{15}$$

We assume that the network $G(V, E)$ is divided into two parts: $M \subseteq V$ and $\bar{M} = V \setminus M$. The elements of x represent whether a node i belongs to the set M or not: $x_i = +1$ if node i belongs to the set M ; otherwise, $x_i = -1$. GND follows the standard relaxation from the integer constraint $x_i \in \{+1, -1\}$ to $x_i \in \mathcal{R}$. The solution to this relaxed constrained

minimization problem is given by the second-smallest eigenvector of the node-weighted Laplacian $\lambda_2 x^{(2)} = L_w x^{(2)}$. For each step, GND removes all of the nodes i whose corresponding value in the second-smallest eigenvector is nonnegative ($x_i^{(2)} \geq 0$) and has a neighbor j with a negative entry ($x_j^{(2)} < 0$). Ultimately, the network will fragment into two subnetworks M and \bar{M} . It achieves high performance by combining the approximation spectrum of the Laplace operator with a fine-tuning mechanism associated with the weighted vertex cover problem.

Cycle-Tree-Guided-Attack (CTGA) The CTGA algorithm [65], based on the tree-packing model [48], extends the original model to the k -core attack problem by allowing different tree components to be adjacent to each other and permitting additional edges within each tree component. The algorithm iteratively determines the removal probability of nodes using a coarse-grained vertex state represented in groups of four and removes nodes one by one starting with those having the highest removal probability.

Supplementary Materials: The following supporting information can be downloaded at: <https://www.mdpi.com/article/10.3390/e26030248/s1>, Reference [69] is cited in the supplementary materials.

Author Contributions: P.P., T.F., and L.L. conceived the idea, designed the research framework, and discussed the results. P.P. collected the data, conducted the study, and drafted the initial manuscript. T.F. refined the design and experiments, and revised the manuscript. T.F. and L.L. supervised the research and performed the final manuscript editing. All authors reviewed and confirmed the methods and conclusions. All authors have read and agreed to the published version of the manuscript.

Funding: This research was funded by the National Natural Science Foundation of China (Grant No. T2293771), support from the STI 2030–Major Projects (2022ZD0211400), and the New Cornerstone Science Foundation through the XPLOER PRIZE.

Data Availability Statement: The data and code used in this work are available on request from the authors.

Acknowledgments: The authors express sincere gratitude to Haijun Zhou for providing the CTGA algorithm code and thank Liming Pan for insightful suggestions.

Conflicts of Interest: The authors declare no conflicts of interest.

References

1. Albert, R.; Jeong, H.; Barabási, A.L. Error and attack tolerance of complex networks. *Nature* **2000**, *406*, 378–382. [[CrossRef](#)]
2. Morone, F.; Makse, H.A. Influence Maximization in Complex Networks through Optimal Percolation. *Nature* **2015**, *524*, 65–68. [[CrossRef](#)]
3. Lü, L.; Zhou, T. Link prediction in complex networks: A survey. *Physica A Stat. Mech. Appl.* **2011**, *390*, 1150–1170. [[CrossRef](#)]
4. Clusella, P.; Grassberger, P.; Pérez-Reche, F.J.; Politi, A. Immunization and targeted destruction of networks using explosive percolation. *Phys. Rev. Lett.* **2016**, *117*, 208301. [[CrossRef](#)]
5. Lü, L.; Chen, D.; Ren, X.L.; Zhang, Q.M.; Zhang, Y.C.; Zhou, T. Vital nodes identification in complex networks. *Phys. Rep.* **2016**, *650*, 1–63. [[CrossRef](#)]
6. Cohen, R.; Erez, K.; Ben-Avraham, D.; Havlin, S. Breakdown of the internet under intentional attack. *Phys. Rev. Lett.* **2001**, *86*, 3682. [[CrossRef](#)] [[PubMed](#)]
7. Braunstein, A.; Dall’Asta, L.; Semerjian, G.; Zdeborová, L. Network Dismantling. *Proc. Natl. Acad. Sci. USA* **2016**, *113*, 12368–12373. [[CrossRef](#)] [[PubMed](#)]
8. Schneider, C.M.; Moreira, A.A.; Andrade, J.S.; Havlin, S.; Herrmann, H.J. Mitigation of Malicious Attacks on Networks. *Proc. Natl. Acad. Sci. USA* **2011**, *108*, 3838–3841. [[CrossRef](#)] [[PubMed](#)]
9. Ren, X.L.; Gleinig, N.; Helbing, D.; Antulov-Fantulin, N. Generalized Network Dismantling. *Proc. Natl. Acad. Sci. USA* **2019**, *116*, 6554–6559. [[CrossRef](#)] [[PubMed](#)]
10. Krebs, V.E. Mapping networks of terrorist cells. *Connections* **2002**, *24*, 43–52.
11. Yan, G.; Vértés, P.E.; Towilson, E.K.; Chew, Y.L.; Walker, D.S.; Schafer, W.R.; Barabási, A.L. Network control principles predict neuron function in the *Caenorhabditis elegans* connectome. *Nature* **2017**, *550*, 519–523. [[CrossRef](#)] [[PubMed](#)]
12. Lehár, J.; Krueger, A.; Zimmermann, G.; Borisy, A. High-order combination effects and biological robustness. *Mol. Syst. Biol.* **2008**, *4*, 215. [[CrossRef](#)] [[PubMed](#)]

13. Morone, F.; Del Ferraro, G.; Makse, H.A. The K-Core as a Predictor of Structural Collapse in Mutualistic Ecosystems. *Nat. Phys.* **2019**, *15*, 95–102. [[CrossRef](#)]
14. Wu, A.K.; Tian, L.; Liu, Y.Y. Bridges in complex networks. *Phys. Rev. E* **2018**, *97*, 012307. [[CrossRef](#)] [[PubMed](#)]
15. Requião da Cunha, B.; González-Avella, J.C.; Gonçalves, S. Fast fragmentation of networks using module-based attacks. *PLoS ONE* **2015**, *10*, e0142824. [[CrossRef](#)] [[PubMed](#)]
16. Musciotto, F.; Miccichè, S. Exploring the landscape of dismantling strategies based on the community structure of networks. *Sci. Rep.* **2023**, *13*, 14448. [[CrossRef](#)]
17. Peng, P.; Fan, T.; Ren, X.L.; Lü, L. Unveiling Explosive Vulnerability of Networks through Edge Collective Behavior. *arXiv* **2023**, arXiv:2310.06407
18. Lambiotte, R.; Rosvall, M.; Scholtes, I. From Networks to Optimal Higher-Order Models of Complex Systems. *Nat. Phys.* **2019**, *15*, 313–320. [[CrossRef](#)]
19. Battiston, F.; Cencetti, G.; Iacopini, I.; Latora, V.; Lucas, M.; Patania, A.; Young, J.G.; Petri, G. Networks beyond Pairwise Interactions: Structure and Dynamics. *Phys. Rep.* **2020**, *874*, 1–92. [[CrossRef](#)]
20. Sanchez-Gorostiaga, A.; Bajić, D.; Osborne, M.L.; Poyatos, J.F.; Sanchez, A. High-order interactions distort the functional landscape of microbial consortia. *PLoS Biol.* **2019**, *17*, e3000550. [[CrossRef](#)]
21. Yu, S.; Yang, H.; Nakahara, H.; Santos, G.S.; Nikolić, D.; Plenz, D. Higher-Order Interactions Characterized in Cortical Activity. *J. Neurosci.* **2011**, *31*, 17514–17526. [[CrossRef](#)]
22. Alvarez-Rodriguez, U.; Battiston, F.; de Arruda, G.F.; Moreno, Y.; Perc, M.; Latora, V. Evolutionary dynamics of higher-order interactions in social networks. *Nat. Hum. Behav.* **2021**, *5*, 586–595. [[CrossRef](#)]
23. Grilli, J.; Barabás, G.; Michalska-Smith, M.J.; Allesina, S. Higher-Order Interactions Stabilize Dynamics in Competitive Network Models. *Nature* **2017**, *548*, 210–213. [[CrossRef](#)] [[PubMed](#)]
24. Myers, C.R. Software Systems as Complex Networks: Structure, Function, and Evolvability of Software Collaboration Graphs. *Phys. Rev. E* **2003**, *68*, 046116. [[CrossRef](#)]
25. Battiston, F.; Amico, E.; Barrat, A.; Bianconi, G.; Ferraz de Arruda, G.; Franceschiello, B.; Iacopini, I.; Kéfi, S.; Latora, V.; Moreno, Y.; et al. The Physics of Higher-Order Interactions in Complex Systems. *Nat. Phys.* **2021**, *17*, 1093–1098. [[CrossRef](#)]
26. Zhang, Y.; Lucas, M.; Battiston, F. Higher-order interactions shape collective dynamics differently in hypergraphs and simplicial complexes. *Nat. Commun.* **2023**, *14*, 1605. [[CrossRef](#)]
27. Milo, R.; Shen-Orr, S.; Itzkovitz, S.; Kashtan, N.; Chklovskii, D.; Alon, U. Network motifs: Simple building blocks of complex networks. *Science* **2002**, *298*, 824–827. [[CrossRef](#)] [[PubMed](#)]
28. Spirin, V.; Mirny, L.A. Protein complexes and functional modules in molecular networks. *Proc. Natl. Acad. Sci. USA* **2003**, *100*, 12123–12128. [[CrossRef](#)]
29. Benson, A.R.; Gleich, D.F.; Leskovec, J. Higher-Order Organization of Complex Networks. *Science* **2016**, *353*, 163–166. [[CrossRef](#)]
30. Sizemore, A.E.; Giusti, C.; Kahn, A.; Vettel, J.M.; Betzel, R.F.; Bassett, D.S. Cliques and cavities in the human connectome. *J. Comput. Neurosci.* **2018**, *44*, 115–145. [[CrossRef](#)]
31. Giusti, C.; Pastalkova, E.; Curto, C.; Itskov, V. Clique Topology Reveals Intrinsic Geometric Structure in Neural Correlations. *Proc. Natl. Acad. Sci. USA* **2015**, *112*, 13455–13460. [[CrossRef](#)]
32. Lu, Y.; Huang, Y.; Li, T. More is Different: Constructing the Most Comprehensive Human Protein High-Order Interaction Dataset. *bioRxiv* **2023**. [[CrossRef](#)]
33. Marsh, J.A.; Teichmann, S.A. Structure, dynamics, assembly, and evolution of protein complexes. *Annu. Rev. Biochem.* **2015**, *84*, 551–575. [[CrossRef](#)]
34. Bairey, E.; Kelsic, E.D.; Kishony, R. High-Order Species Interactions Shape Ecosystem Diversity. *Nat. Commun.* **2016**, *7*, 12285. [[CrossRef](#)]
35. Mayfield, M.M.; Stouffer, D.B. Higher-Order Interactions Capture Unexplained Complexity in Diverse Communities. *Nat. Ecol. Evol.* **2017**, *1*, 0062. [[CrossRef](#)]
36. Pattison, P.; Robins, G. Neighborhood-based models for social networks. *Sociol. Methodol.* **2002**, *32*, 301–337. [[CrossRef](#)]
37. Majhi, S.; Perc, M.; Ghosh, D. Dynamics on higher-order networks: A review. *J. R. Soc. Interface* **2022**, *19*, 20220043. [[CrossRef](#)]
38. Kavitha, T.; Liebchen, C.; Mehlhorn, K.; Michail, D.; Rizzi, R.; Ueckerdt, T.; Zweig, K.A. Cycle bases in graphs characterization, algorithms, complexity, and applications. *Comput. Sci. Rev.* **2009**, *3*, 199–243. [[CrossRef](#)]
39. Fan, T.; Lü, L.; Shi, D.; Zhou, T. Characterizing cycle structure in complex networks. *Commun. Phys.* **2021**, *4*, 272. [[CrossRef](#)]
40. Zhang, W.; Li, W.; Deng, W. The characteristics of cycle-nodes-ratio and its application to network classification. *Commun. Nonlinear Sci. Numer. Simul.* **2021**, *99*, 105804. [[CrossRef](#)]
41. Zdeborová, L.; Zhang, P.; Zhou, H.J. Fast and simple decycling and dismantling of networks. *Sci. Rep.* **2016**, *6*, 37954. [[CrossRef](#)]
42. Goltsev, A.V.; Dorogovtsev, S.N.; Mendes, J.F.F. k-core (bootstrap) percolation on complex networks: Critical phenomena and nonlocal effects. *Phys. Rev. E* **2006**, *73*, 056101. [[CrossRef](#)]
43. Dorogovtsev, S.N.; Goltsev, A.V.; Mendes, J.F.F. K-core organization of complex networks. *Phys. Rev. Lett.* **2006**, *96*, 040601. [[CrossRef](#)]
44. Schaub, M.T.; Benson, A.R.; Horn, P.; Lippner, G.; Jadbabaie, A. Random walks on simplicial complexes and the normalized Hodge 1-Laplacian. *SIAM Rev.* **2020**, *62*, 353–391. [[CrossRef](#)]

45. Vega, Y.M.; Vázquez-Prada, M.; Pacheco, A.F. Fitness for synchronization of network motifs. *Phys. A: Stat. Mech. Its Appl.* **2004**, *343*, 279–287. [[CrossRef](#)]
46. Iacopini, I.; Petri, G.; Barrat, A.; Latora, V. Simplicial models of social contagion. *Nat. Commun.* **2019**, *10*, 2485. [[CrossRef](#)] [[PubMed](#)]
47. Derényi, I.; Palla, G.; Vicsek, T. Clique percolation in random networks. *Phys. Rev. Lett.* **2005**, *94*, 160202. [[CrossRef](#)] [[PubMed](#)]
48. Zhou, H.J. Spin Glass Approach to the Feedback Vertex Set Problem. *Eur. Phys. J. B* **2013**, *86*, 455. [[CrossRef](#)]
49. Mugisha, S.; Zhou, H.J. Identifying Optimal Targets of Network Attack by Belief Propagation. *Phys. Rev. E* **2016**, *94*, 012305. [[CrossRef](#)] [[PubMed](#)]
50. Shi, D.; Chen, Z.; Sun, X.; Chen, Q.; Ma, C.; Lou, Y.; Chen, G. Computing cliques and cavities in networks. *Commun. Phys.* **2021**, *4*, 249. [[CrossRef](#)]
51. Sanei-Mehri, S.V.; Das, A.; Tirthapura, S. Enumerating top-k quasi-cliques. In Proceedings of the 2018 IEEE International Conference on Big Data (Big Data), Seattle, WA, USA, 10–13 December 2018; pp. 1107–1112.
52. Balasundaram, B.; Butenko, S.; Hicks, I.V. Clique relaxations in social network analysis: The maximum k-plex problem. *Oper. Res.* **2011**, *59*, 133–142. [[CrossRef](#)]
53. Shi, D.; Chen, G.; Thong, W.W.K.; Yan, X. Searching for optimal network topology with best possible synchronizability. *IEEE Circuits Syst. Mag.* **2013**, *13*, 66–75. [[CrossRef](#)]
54. Yeger-Lotem, E.; Sattath, S.; Kashtan, N.; Itzkovitz, S.; Milo, R.; Pinter, R.Y.; Alon, U.; Margalit, H. Network motifs in integrated cellular networks of transcription–regulation and protein–protein interaction. *Proc. Natl. Acad. Sci. USA* **2004**, *101*, 5934–5939. [[CrossRef](#)] [[PubMed](#)]
55. Alon, U. Network motifs: Theory and experimental approaches. *Nat. Rev. Genet.* **2007**, *8*, 450–461. [[CrossRef](#)] [[PubMed](#)]
56. Rives, A.W.; Galitski, T. Modular organization of cellular networks. *Proc. Natl. Acad. Sci. USA* **2003**, *100*, 1128–1133. [[CrossRef](#)] [[PubMed](#)]
57. Bettencourt, L.M.; Gintautas, V.; Ham, M.I. Identification of functional information subgraphs in complex networks. *Phys. Rev. Lett.* **2008**, *100*, 238701. [[CrossRef](#)] [[PubMed](#)]
58. Itzkovitz, S.; Alon, U. Subgraphs and network motifs in geometric networks. *Phys. Rev. E* **2005**, *71*, 026117. [[CrossRef](#)] [[PubMed](#)]
59. Newman, M. *Networks*; Oxford University Press: Oxford, UK, 2018.
60. Barabasi, A.L.; Albert, R. Emergence of Scaling in Random Networks. *Science* **1999**, *286*, 509–512. [[CrossRef](#)] [[PubMed](#)]
61. Jeong, H.; Mason, S.P.; Barabási, A.L.; Oltvai, Z.N. Lethality and centrality in protein networks. *Nature* **2001**, *411*, 41–42. [[CrossRef](#)]
62. Rossi, R.; Ahmed, N. The Network Data Repository with Interactive Graph Analytics and Visualization. *Proc. AAAI Conf. Artif. Intell.* **2015**, *29*, 2492–2493. [[CrossRef](#)]
63. Cheng, X.Q.; Ren, F.X.; Shen, H.W.; Zhang, Z.K.; Zhou, T. Bridgeness: A Local Index on Edge Significance in Maintaining Global Connectivity. *J. Stat. Mech. Theory Exp.* **2010**, *2010*, P10011. [[CrossRef](#)]
64. Girvan, M.; Newman, M.E. Community Structure in Social and Biological Networks. *Proc. Natl. Acad. Sci.* **2002**, *99*, 7821–7826. [[CrossRef](#)]
65. Zhou, H.J. Cycle-Tree Guided Attack of Random K-core: Spin Glass Model and Efficient Message-Passing Algorithm. *Sci. China Physics. Mech. Astron.* **2022**, *65*, 230511. [[CrossRef](#)]
66. Zhao, D.; Li, R.; Peng, H.; Zhong, M.; Wang, W. Higher-order percolation in simplicial complexes. *Chaos Solitons Fractals* **2022**, *155*, 111701. [[CrossRef](#)]
67. Sharma, A.; Vanjani, P.; Paliwal, N.; Basnayaka, C.M.W.; Jayakody, D.N.K.; Wang, H.C.; Muthuchidambaranathan, P. Communication and networking technologies for UAVs: A survey. *J. Netw. Comput. Appl.* **2020**, *168*, 102739. [[CrossRef](#)]
68. Xu, J.J.; Chen, H. Fighting organized crimes: Using shortest-path algorithms to identify associations in criminal networks. *Decis. Support Syst.* **2004**, *38*, 473–487. [[CrossRef](#)]
69. Holland, P.W.; Laskey, K.B.; Leinhardt, S. Stochastic blockmodels: First steps. *Soc. Netw.* **1983**, *5*, 109–137. [[CrossRef](#)]

Disclaimer/Publisher’s Note: The statements, opinions and data contained in all publications are solely those of the individual author(s) and contributor(s) and not of MDPI and/or the editor(s). MDPI and/or the editor(s) disclaim responsibility for any injury to people or property resulting from any ideas, methods, instructions or products referred to in the content.